Engineering

Electrical Engineering fields

Okayama University *Year* 2002

An application of sensorless drive technology to a three-phase hybrid stepping motor drive

Satoshi Ogasawara
Okayama University

An Application of Sensorless Drive Technology to a Three-Phase Hybrid Stepping Motor Drive

Satoshi Ogasawara
Department of Electrical Engineering, Okayama University
3-1-1 Tsushima-Naka, Okayama, 700 JAPAN

Abstract— **This paper presents a three-phase hybrid stepping motor drive system to which sensorless drive technology of brushless dc motors is applied. The drive system is characterized by measurement of back emf in the motor windings. As a result, the drive system can damp rotor natural vibration of the three-phase hybrid stepping motor. Moreover, an acceleration and deceleration pattern is proposed to suppress undesirable transient vibration in acceleration, deceleration, and positioning operations. Some experimental results show that the experimental system can damp the rotor natural vibration even if the rotor inertia varies.**

I. Introduction

Numerous stepping motors are widely used in office automation or factory automation apparatus, because of low cost and easy positioning. However, a stepping motor drived by the constant-current open-loop control has a big problem that a large natural vibration in the motor rotor occurs, because commutations of the motor current are performed regardless of the rotor position. It has pointed out that a commutation at the optimum timing, which corresponds to half of the natural vibration, makes it possible to suppress the undesirable vibration in two-step response[1]. However, in order to obtain good suppression characteristics of the natural vibration, it is necessary to previously know the period of the natural vibration, and to accurately adjust the control circuit. Moreover, readjustment is required when the driving condition varies, because the period of the natural vibration depends on the rotor inertia and the motor current.

This paper presents an application of sensorless drive technology to a three-phase hybrid stepping motor drive system. The drive system is characterized by sensorless detection of the rotating direction based on measurement of back emf in the motor windings. As a result, the drive system can damp rotor natural vibration of the three-phase hybrid stepping motor. Moreover, an acceleration and deceleration pattern is derived from a simple model of the rotor vibration, to suppress undesirable transient vibration in acceleration, deceleration, and positioning operations. An experimental drive system has been implemented and tested to confirm the effectiveness and versatility of the proposed pattern. Some experimental results show that the experimental system can damp the rotor natural vibration even if the rotor inertia varies. Comparing with the conventional pattern, it is confirmed that the proposed pattern has great contribution to damp the undesirable vibration.

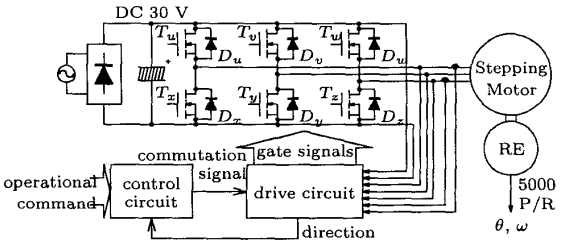

Fig. 1. System configuration.

TABLE I
Parameters of three-phase hybrid stepping motor.

step angle	1.58	deg
voltage	5.3	V
current	0.5	A
resistance	2.65	Ω
inductance	1.58	mH
holding torque (at 0.5 A)	700	gcm
moment of inertia	79.67	gcm^2

II. System Configuration

Fig. 1 shows the proposed system configuration of a three-phase hybrid stepping motor drive system. The system consists of a three-phase hybrid stepping motor, a voltage-source inverter, a gate drive circuit, and a control circuit. The configuration is almost the same as the conventional open-loop drive system in which the motor currents are regulated constantly. Note that the gate drive circuit includes an additional circuit which can detect the rotating direction of the rotor based on the back emf in the motor windings. The circuit takes in the voltage signals between two terminals of the flywheeling diodes, because the back emf makes these diodes in a phase turn on even if no gate signal applies to the two MOSFET's in the phase. The additional circuit is the same as the detection circuit of a position sensorless brushless dc motor drive[2]. The circuit informs the control circuit that the rotating direction is altered by the rotor natural vibration.

The control circuit, which is implemented in a one-chip microprocessor (PIC16F84), can measure the period of the rotor natural vibration from the direction signal. The controller receives operational commands through a serial interface and generates the optimum commutation signals taking the measured period into account. Table I shows

0-7803-7156-9/02/$10.00© 2002 IEEE

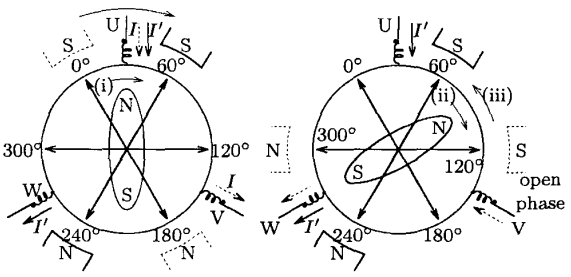

Fig. 2. Natural vibration of rotor.

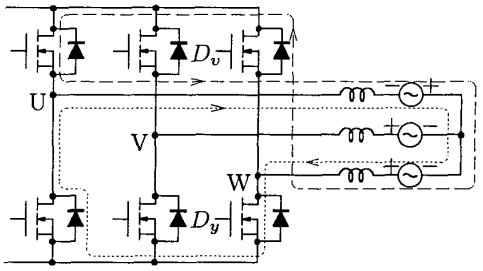

Fig. 3. Principle of sensorless detection of rotating direction.

the motor parameters of the three-phase hybrid stepping motor used in the experimental system. A rotary encoder (RE) is connected to the motor shaft for measurement of the rotor position θ and the rotor speed ω. However, the rotor position and speed signals are not used in the drive system.

III. Natural Vibration of Rotor

A. Principle of Natural Vibration

Fig. 2 shows a process of the rotor natural vibration existing in a three-phase hybrid stepping motor. The stepping motor is represented as a two-pole permanent magnet synchronous machine, because of equivalence to a polyphase synchronous machine in electrical characteristics. At first, it is assumed that the motor current I flows from U-phase to V-phase, which is shown as broken-line arrows in Fig. 2(a). It is equivalent that magnets shown by the broken lines exist at a position of 0 deg.

Secondly, the V-phase current is commutated to W-phase winding as shown by solid-line arrows, and then position of the equivalent magnets changes from 0 deg to 60 deg. A magnetic attraction between the rotor and the equivalent magnet make the rotor accelerate clockwise as shown by arrow (i). When the rotor reaches the same position as the equivalent magnet, kinetic energy stored in the rotor inertia force the rotor to rotate clockwise though the acceleration torque becomes zero. After that, the rotor is decelerated by the magnetic attraction, as shown in Fig. 2(b)(ii), and the rotating direction is reversed near the point of 120 deg. Since the magnetic attraction makes the rotor accelerate counterclockwise again as shown by arrow (iii), the rotor continues the natural vibration and comes to a standstill at last.

When the rotating direction alters, a commutation of motor current from U-phase to V-phase makes it possible to settle the rotor at 120 deg without the natural vibration, because the rotor has no kinetic energy and the rotor position is almost 120 deg. It is an easy way to suppress the rotor natural vibration. However, it is not easy to give a commutation signal at the optimum timing. In order to solve this problem, a sensorless drive technology developed for brushless dc motors[2] is introduced into the three-phase hybrid stepping motor drive system.

When the motor current flows from U-phase to W-phase, V-phase is a so-called "open phase" in which both the upper- and lower-side MOSFET's are turned off. In Fig. 2(b), distance between the rotor N-pole and the V-phase, i.e., open phase, winding decreases in case (ii), but increases in case (iii). Therefore, an alternation appears in polarity of the induced emf of the V-phase winding when the rotating direction is reversed. The polarity of the induced emf can be detected by applying the sensorless drive technology, because the control circuit of the sensorless brushless dc motor estimates the rotor position based on the back emf induced in the open-phase winding.

B. Sensorless Detection of Rotating Direction

Fig. 3 shows principle of the sensorless detection of the rotating direction. The motor current flows from U-phase to W-phase, and the rotor N-pole gets closer to the V-phase winding, as shown in Fig. 2(b)(ii). In this case, each phase winding induces a back emf, the polarity of which is indicated in Fig. 3, and then conversion from mechanical energy to electrical energy makes the rotor decelerate. The U- and W-phase devices perform switching operation so that the motor current is kept constant, but the V-phase devices continue to be off state. The broken or dotted line in Fig. 3 indicates the current flow in the case that the U- and W-phase motor terminals are shorted to the upper side or lower side of the dc link, respectively. In the current regulation, the two switching states are used repeatedly.

Since the U- and W-phase terminals are shorted by the switching devices, the three-phase induced voltages force the potential of the V-phase terminal to be higher than the shorted point. Therefore, diode D_v turns on when the two terminals are shorted to upper side of the dc link, though the two V-phase diodes continue to be off-state when the two terminals are shorted to lower side of the dc link.

On the other hand, reverse of the rotating direction changes the polarity of each induced voltage. In this case, the potential of the V-phase terminal is lower than the shorted point. Therefore, diode D_y turns on when the two terminals are shorted to lower side of the dc link, though the two diodes in V-phase continue to be off-state when the two terminals are shorted to upper side of the dc link.

As mentioned above, the three-phase induced voltages

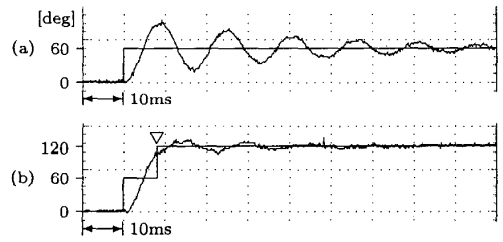

Fig. 4. Position response.

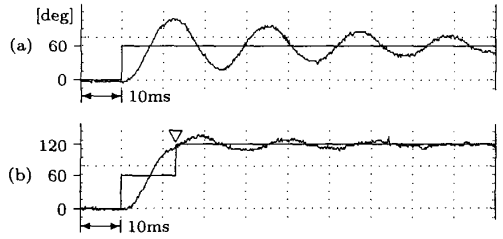

Fig. 5. Variation of inertia.

cause a small current through a diode even in the V-phase that both switching devices are off state. Moreover, the diode through which the small current flows depends on the rotating direction. Therefore, it is possible to detect the rotating direction by checking the conducting mode of the diodes through which the small current flows. The conducting mode of a diode can be judged from the forward voltage.

C. Reduction of Natural Vibration

Fig. 4 shows experimental position responses of the three-phase hybrid stepping motor. A rotary encoder mounted on the rotor shaft is used for the measurement of the rotor position. In the one-step response (a), after a commutation, the rotor settles to the position of 60 deg accompanied by a large vibration. The natural vibration has a bad influence on the position control of the stepping motor. As mentioned above, at the peak point, the rotor position reaches almost 120 deg, and the rotor speed becomes zero. In the two-step response (b), the position response in an interval between the first and second commutations is the same as that of (a). However, the rotor position settles to 120 deg accompanied by a small vibration. Note that the second commutation marked by $\bigtriangledown$ is generated by detecting the induced emf in the open phase. The settling time in the two-step response is much shorter than that in the one-step response.

Fig. 5 shows experimental position responses in the case that the rotor inertia is increased to 2.5 times. Compared with Fig. 4, it is shown that the period of the natural vibration is increased to 1.5 times in the one-step response. However, similarly to Fig. 4(b), the most part of the natural vibration after the second commutation is suppressed in the two-step response. The experimental results conclude that the proposed drive system can suppress the natural

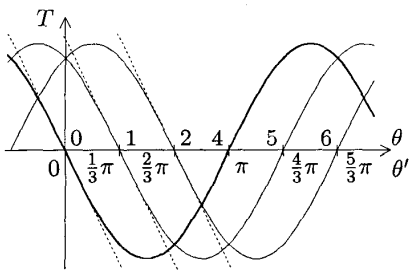

Fig. 6. Relationship between rotor position and torque.

vibration even if the period is changed by any parameter variation.

It is notable that measurement of the time interval between the first and second commutations makes it possible to know the period of the natural vibration, because the interval corresponds to half of the period. In the next section, a new generation method of the commutation signals will be proposed.

IV. A New Generation Method of Commutation Signals

A. Modeling of Three-Phase Hybrid Stepping Motor

Fig. 6 shows relationship between the rotor position and torque of a three-phase hybrid stepping motor. In the case that the motor current is kept constant, the motor torque is sinusoidal with respect to the rotor position. A commutation makes the torque characteristics move by $\pi/3$ in electrical angle. Since the one-step position response shown in Fig. 4 or Fig. 5 is an almost ideal damped vibration, the torque characteristic can be linearized as shown by the dotted lines in Fig. 6. For simplicity, mechanical friction is neglected. In this case, the equation of motion for the rotor can be expressed by

$$J\frac{d^2}{dt^2}\theta'(t) = -k\theta'(t), \tag{1}$$

where $\theta'(t)$ [rad], J [kgm^2] and k [Nm/rad] mean the rotor position, the rotor inertia and the stiffness, respectively. Normalizing the rotor position with one step derives the following equations:

$$\theta(t) = \frac{\theta'(t)}{\pi/3} \tag{2}$$

$$\frac{d^2}{dt^2}\theta(t) + \beta^2\theta(t) = 0 \tag{3}$$

where $\beta = \sqrt{k/J}$ is the angular frequency of the natural vibration. Taking the initial position $\theta(0)$ and the initial speed $\omega(0)$ in consideration, Laplace transformation of the above equation gives

$$\Theta(s) = \frac{s\theta(0) + \omega(0)}{s^2 + \beta^2}. \tag{4}$$

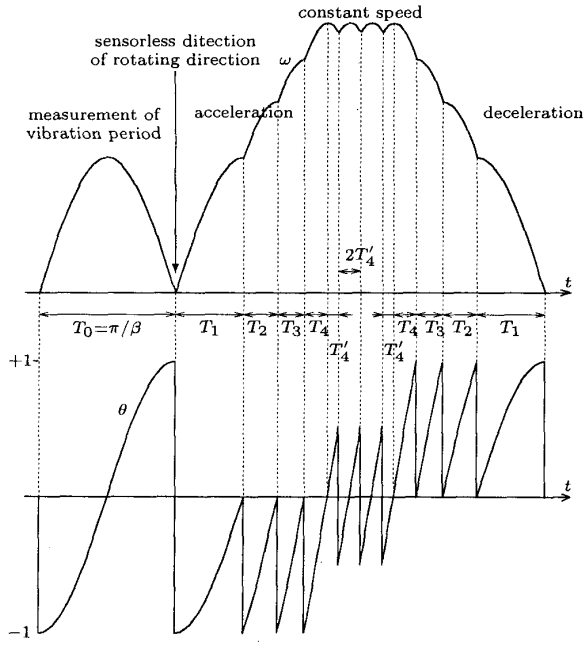

Fig. 7. Proposed pattern for acceleration and deceleration.

Therefore, the solution of the equation of motion is given by

$$\left.\begin{aligned}\theta(t) &= \theta(0)\cos\beta t + \frac{\omega(0)}{\beta}\sin\beta t \\ \omega(t) &= -\beta\theta(0)\sin\beta t + \omega(0)\cos\beta t.\end{aligned}\right\} \tag{5}$$

On the other hand, natural vibration after a commutation can be analyzed by using a substitution of initial values. For example, the following substitution is available in the case that one-step commutation toward positive direction occurs at t_1.

$$\left.\begin{aligned} t &\longleftarrow t - t_1 \\ \theta(0) &\longleftarrow \theta(t_1) - 1 \\ \omega(0) &\longleftarrow \omega(t_1)\end{aligned}\right\} \tag{6}$$

B. Acceleration Operation

Assuming that the rotor begins to rotate by one-step commutation toward positive direction from standstill, the initial position and speed are $\theta(0) = -1$ and $\omega(0) = 0$, respectively. From (5), the position response $\theta_1(t)$ and the speed response $\omega_1(t)$ is given by

$$\left.\begin{aligned}\theta_1(t) &= -\cos\beta t \\ \omega_1(t) &= \beta\sin\beta t.\end{aligned}\right\} \tag{7}$$

Since the rotor speed reaches the maximum value of β at $t = T_1$, a next commutation at this timing contributes to smooth acceleration.

$$T_1 = \frac{\pi}{2\beta} \tag{8}$$

When the second commutation is performed at T_1, the initial position and speed are substituted as $\theta_2(0) = -1$ and $\omega_2(0) = \beta$, respectibely. Therefore, the position response $\theta_2(t)$ and the speed response $\omega_2(t)$ after the second commutation are calculated by (??).

$$\left.\begin{aligned}\theta_2(t) &= -\sqrt{2}\cos(\beta t + \frac{\pi}{4}) \\ \omega_2(t) &= \sqrt{2}\beta\sin(\beta t + \frac{\pi}{4})\end{aligned}\right\} \tag{9}$$

Since the rotor speed reaches the maximum value of $\sqrt{2}\beta$ at $t = T_2$ again, the third commutation is performed for the smooth acceleration.

$$T_2 = \frac{\pi}{4\beta} \tag{10}$$

In the case of the n-th commutation, the initial position and the initial speed are $\theta_n(0) = -1$ and $\omega_n(0) = \sqrt{n-1}\beta$, respectively. The position response $\theta_n(t)$, the speed response $\omega_n(t)$ and the commutation interval T_n is expressed as follows.

$$\left.\begin{aligned}\theta_n(t) &= -\sqrt{n}\cos(\beta t + \phi_n) \\ \omega_n(t) &= \sqrt{n}\beta\sin(\beta t + \phi_n) \\ T_n &= \frac{1}{\beta}\phi_n \\ \phi_n &= \sin^{-1}\frac{1}{\sqrt{n}}\end{aligned}\right\} \tag{11}$$

The commutations, each interval of which is calculated by the above equation, make it possible to achieve the smooth acceleration shown in Fig. 7.

C. Constant-Speed Operation

It is important that unnecessary natural vibration can be reduced when the motor operation transfers from acceleration to constant-speed operation. While the motor is accelerating, the average torque is positive because $\theta(t)$ changes between -1 and 0 as shown in Fig. 7. Since the average torque is almost zero in the constant-speed operation, $\theta(t)$ should exist in a range between -0.5 and $+0.5$. For the smooth transfer after the n-th commutation interval T_n, an extra time interval T'_n is inserted before the next commutation as shown in Fig. 7.

$$T'_n = \frac{1}{\beta}\sin^{-1}\frac{1}{2\sqrt{n}} \tag{12}$$

$\theta(t)$ reaches to $+0.5$ when the extra interval is over, and then the next commutation makes $\theta(t)$ change to -0.5. Subsequent commutations for constant-speed operation are made at intervals of $2T'_n$ so that $\theta(t)$ exists between -0.5 and $+0.5$. The extra interval has a great contribution for the smooth transfer to constant-speed operation.

D. Deceleration Operation and Stopping

Deceleration operation is the quite opposite of the acceleration operation. An extra interval T'_n is inserted before the interval of T_n when the motor operation transfers from constant-speed to deceleration. As a result of the extra interval, the motor can generate negative torque immediately, and the motor decelerates without unnecessary

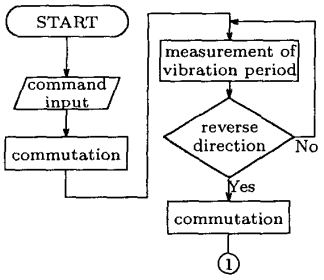

Fig. 8. Program flow for time measurement.

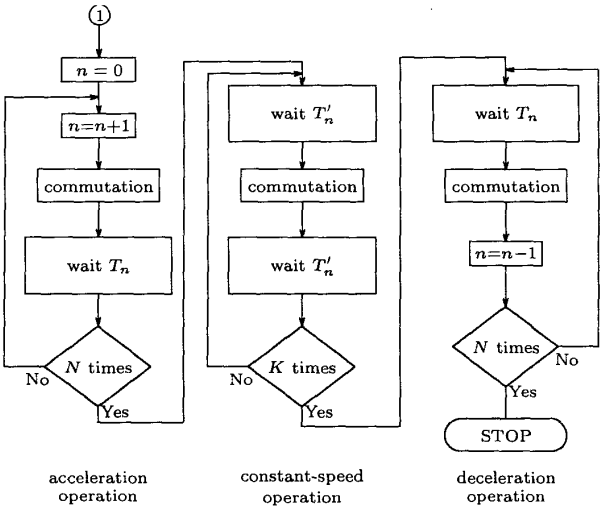

Fig. 9. Program flow for acceleration and deceleration.

natural vibration. Since the curves of the rotor position $\theta(t)$ and the rotor speed $\omega(t)$ in deceleration operation are symmetry with those in acceleration operation as shown in Fig. 7, commutations, each interval of which is calculated by (11), are performed according to n down to 1. Finally, at the end of the interval T_1, the rotor position reachs the goal and the rotor speed $\omega(t)$ become zero. Therefore, the final commutation makes it possible to stop the rotor with no natural vibration.

E. Proposed Pulse Pattern

Fig. 7 shows the proposed acceleration and deceleration pattern. In this case, the rotor rotates 13 steps and stops.

First of all, period of the natural vibration is measured by using the sensorless detection circuit of the rotating direction. When one-step commutation toward positive direction is performed from a standstill, the rotor begins to rotate toward positive direction. After a time interval of T_0 from the first commutation, the natural vibration inverses the rotating direction. Therefore, the controller can measure the interval of T_0, and T_0 corresponds to the half of the vibration period.

$$\beta = \frac{\pi}{T_0} \tag{13}$$

Two-step commutations in an instant that the direction signal is reversed cause the same natural vibration as that after the first commutation. After that, acceleration and deceleration are performed according to the above mentioned method. In Fig. 7, the controller gives the acceleration, constant-speed and deceleration pluses by 4, 3, and 4 steps, respectively. The proposed pulse pattern makes it possible to perform positioning without undesirable natural vibration.

Figs. 8 and 9 show the program flows for generating the proposed pluse pattern. The proposed pattern can rotate the rotor by $2N+K+2$ steps, because two-step commutation is necessary for measurement of the vibration period.

TABLE II
CALCULATION TABLE.

n	$A_n = \frac{1}{\pi}\sin^{-1}\frac{1}{\sqrt{n}}$	$A'_n = \frac{1}{\pi}\sin^{-1}\frac{1}{2\sqrt{n}}$
1	0.5	0.16667
2	0.25	0.11503
3	0.19591	0.09321
4	0.16667	0.08043
5	0.14758	0.07178
6	0.13386	0.06543
7	0.12338	0.06052
8	0.11503	0.05657
9	0.10817	0.05330
⋮	⋮	⋮

In the experimental system shown in Fig. 1, a one-chip microprocessor PIC16F84 executes the control program. Eqs. (11) and (12) can be rewritten as follows:

$$\left.\begin{aligned} T_n &= \frac{T_0}{\pi}\sin^{-1}\frac{1}{\sqrt{n}} = A_n T_0 \\ T'_n &= \frac{T_0}{\pi}\sin^{-1}\frac{1}{2\sqrt{n}} = A'_n T_0. \end{aligned}\right\} \tag{14}$$

The proposed pulse generation is characterized by the fact that the required parameters are only n and T_0 and that T_0 can be measured by using the sensorless detection of the rotating direction. Since the calculation table of A_n and A'_n shown in Table II is stored in the memory, T_n or T'_n can be calculated easily as a product of T_0 and a value in the table.

V. Experimental Results

A. Conventional Pulse Pattern

Fig. 10 shows a conventional pulse pattern having trapezoidal shape for acceleration and deceleration. In the experimental system, a pulse control LSI PCL-3AM(Nippon

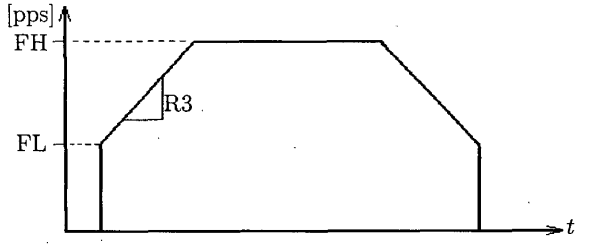

Fig. 10. Conventional pattern for acceleration and deceleration.

Pulse Motor) is used for pulse generation of the conventional pattern. The LSI can generate the trapezoidal pulse pattern according to the following parameters: starting frequency FL, top frequency FH, acceleration rate R3, and moving pulse number R0.

Fig. 11 shows a transient response when the conventional pulse pattern puts the position of the stepping motor forward by 14 steps. Here, the rotor position $\theta(t)$ is shown in a range from 0 to 2π in electrical angle, and rise and fall in the commutation signal indicate that a commutation is performed. In order to compare the experimental result with that of the proposed pattern shown in Fig. 13, the parameters of the trapezoidal pattern are set up as FL=170 pps, FH=596 pps, and R3=44.4 pps/ms, respectively. Since the pulse control LSI generates the commutation pulses regardless of the rotor position, a large natural vibration occurs after commutations. The vibration continues for a long time more than 60 ms, even though no commutation signal is applied.

Fig. 12 shows a transient response in the case that the inertia increases to 2.5 times. The same pulse pattern as that in Fig. 11 drives the stepping motor, because the controller can not know the change of the inertia. The experimental result shows that the rotor falls out of step with the commutation signal. In the case of Fig. 12, the rotor came to a standstill with an excessive rotation by 18 steps. The experimental results conclude that it is required not only to adjust the pattern parameters carefully but also to readjust it when the inertia varies.

B. Proposed Pulse Pattern

Fig. 13 shows a transient response when the proposed pulse pattern is introduced to the experimental system. The pattern also advances the rotor position by 14 steps. At the time indicated by a line, the rotating direction changes, and the directional detection signal is given from the motor voltages. The period of the natural vibration is measured as a time interval from the first commutation to the detected signal. The proposed pulse pattern is generated by a one-chip microprocessor, taking the measured period of the natural vibration in consideration. Since almost no undesirable vibration appears in the positioning operation, the proposed pattern has a great contribution to damp the natural vibration.

Fig. 14 shows a transient response when the inertia increases to 2.5 times. Compared with Fig. 12, the rotor

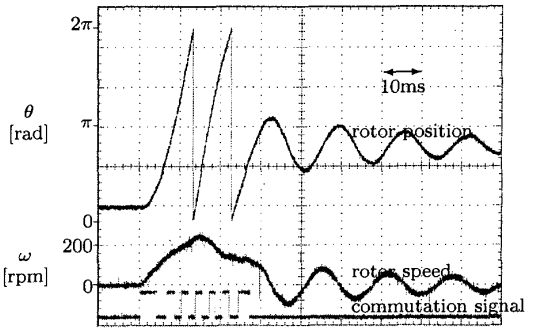

Fig. 11. Performance of conventional pattern.

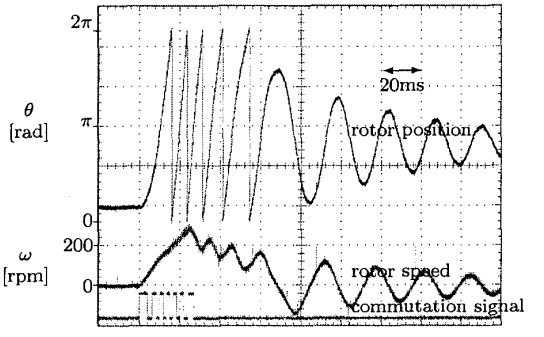

Fig. 12. Performance of conventional pattern (inertia: 2.5 times).

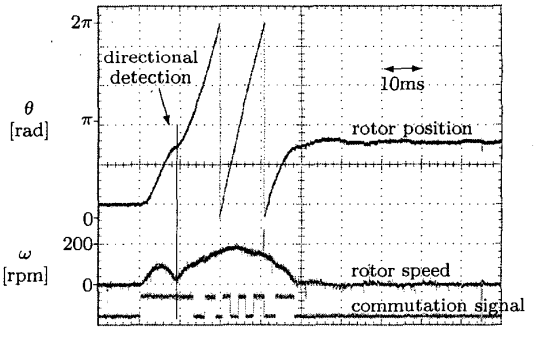

Fig. 13. Performance of proposed pattern.

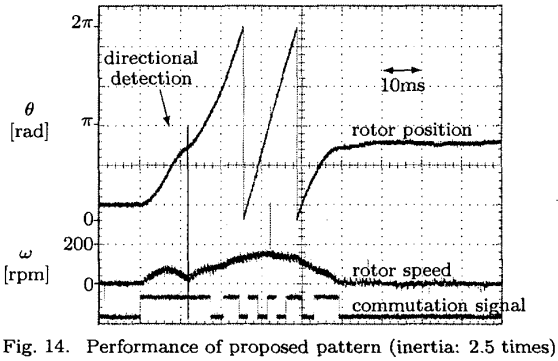

Fig. 14. Performance of proposed pattern (inertia: 2.5 times).

keeps synchronism with the commutation signal. Although the period of the natural vibration increases to 1.5 times, undesirable vibration is suppressed almost completely. The experimental result indicates that good transient responses can be obtained with no adjustment even if the inertia varies, because the period of the natural vibration is measured each time by using sensorless detection of the rotating direction.

C. Modification of Pulse Pattern

When it is known that the inertia is invariable, the measurement of the natural vibration is not necessary at beginning of each positioning operation. The controller of the experimental system can utilize information of the previously measured vibration period.

Fig. 15 shows a transient response of the proposed pulse pattern shown in Fig. 7. In this case, the rotor position is made to advance by 14 steps. After the first commutation, the vibration period is measured and stored to the memory of the controller. Since the pulse generation takes account of the measured period, the experimental system can suppress undesirable natural vibration.

Fig. 16 shows a transient response in the case that the controller generates the pulse pattern using the stored information of the vibration period. The pattern advances the rotor by 12 steps, and the response is the same as the latter part of Fig. 15. The experimental result demonstrates that it is not necessary to measure the vibration period when the inertia is invariable, and that almost the same response suppressing undesirable vibration can be obtained.

On the other hand, Fig. 17 shows a conventional one-step response. A commutation causes a large vibration which is continued for a time longer than 70 ms. However, use of the previously measured vibration period makes it possible to suppress the large vibration. Fig. 18 shows a one-step response suppressing natural vibration. After $T_0/3$ from the first forward commutation, the controller makes a reverse commutation, and then a forward commutation is made after $T_0/3$. No vibration occurs after the last commutation. The pulse pattern has a great contribution to suppress the natural vibration.

VI. Conclusion

This paper has presented an application of sensorless drive technology to a three-phase stepping motor drive. Sensorless detection of the rotating direction makes it possible to measure the period of the natural vibration. This paper also has proposed a new pulse pattern which can suppress undesirable vibration in a positioning operation. It has shown experimentally that the experimental system can damp the rotor natural vibration even if the rotor inertia varies.

References

[1] H. Ooki: "Pribciple and Applications of Step Motors," JIKKYO SHUPPAN CO., LTD, 1979, in Japanese.

[2] S. Ogasawara and H. Akagi: "An Approach to Position Sensorless Drive for Brushless DC Motors," *IEEE Trans. on Industry Applications*, Vol. IA-27, No. 5, pp. 928–933, Sep./Oct. 1991.

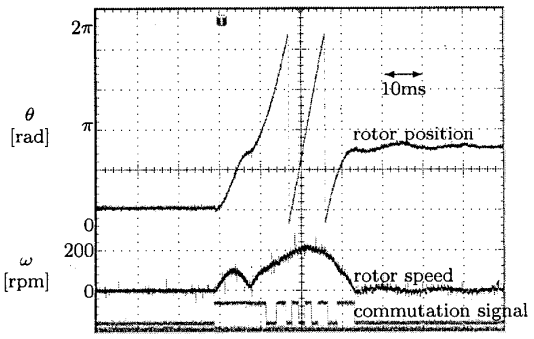

Fig. 15. Position response with measurement of vibration period.

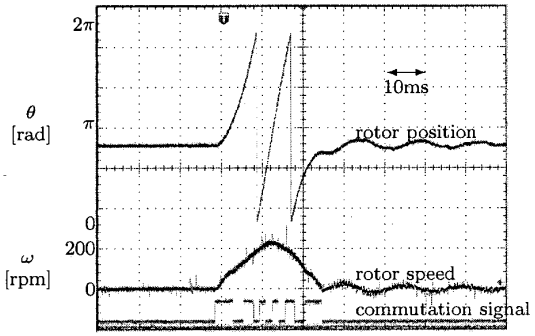

Fig. 16. Position response without measurement of vibration period.

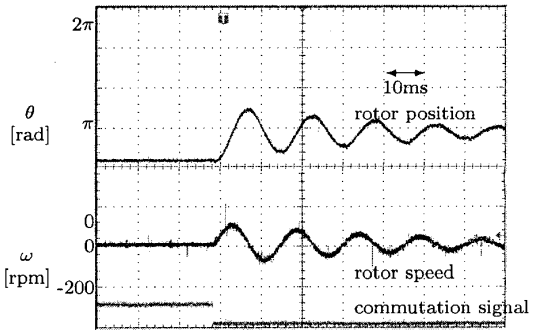

Fig. 17. Conventional one-step response.

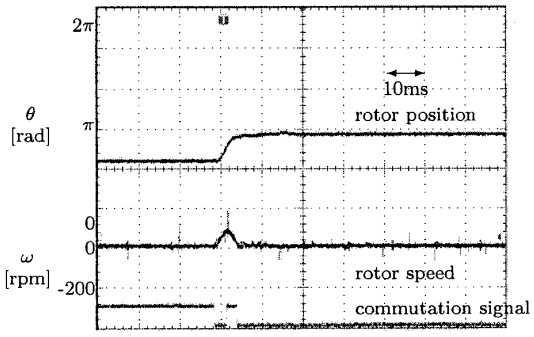

Fig. 18. one-step response suppressing natiral vibration.